JOURNAL OF GEOPHYSICAL RESEARCH, VOL. 101, NO. D7, PAGES 12,567–12,574, MAY 20, 1996

Model study of polar stratospheric clouds and their effect on stratospheric ozone 1. Model description

Anne De Rudder
Center National de Recherches Meteorologiques, Meteo-France, Toulouse, France

Niels Larsen
Division of Middle Atmospheric Research, Danish Meteorological Institute, Copenhagen, Denmark

Xuexi Tie, Guy P. Brassuer, and Claire Granier
National Center for Atmospheric Research, Boulder, Colorado

Abstract. We have included detailed microphysical processes accounting for the formation of polar stratospheric clouds (PSC) into a global chemical/dynamical two-dimensional model to study the effect of heterogeneous reactions occurring on the surface of PSCs on stratospheric ozone. The model explicitly calculates the formation of the PSC particles (50 bin sizes) in terms of heterogeneous nucleation, condensation, and sedimentation. The transport of the particles and heterogeneous reactions on the particles are also represented in the model. The calculated PSC particles show that the distributions of PSCs in the Arctic and in Antarctica are very different. Over Antarctica, nitric acid trihydrate particles (type I PSCs) are formed from early June to late September with a maximum surface area of 15 $\mu m^2/cm^3$, while in the Arctic, type I PSCs are formed only in January with a maximum surface area of 5 $\mu m^2/cm^3$. Ice crystal clouds (type II PSCs) are present over Antarctica in August, but are not seen in the Arctic.

1. Introduction

Although systematic observations of polar stratospheric clouds (PSCs) have been conducted since the 1970s [*McCormick et al.*, 1982; 1985; *McCormick and Trepte*,1986; 1987], it is only in the last 5 to 10 years that the chemical role of these cloud particles has been studied [*Crutzen and Arnold*, 1986; *Toon et al.*, 1986; *Poole and McCormick*, 1988; *Turco et al.*, 1989; *Toon et al.*, 1990; *Larsen*, 1991]. Although the mechanisms are not yet fully understood, it is generally assumed that stratospheric sulfate aerosol particles (SSAs) serve as condensation nuclei for PSC particles [*Crutzen and Arnold*, 1986; *Toon et al.*, 1986]. When the temperature drops below approximately 195 K, HNO_3 and H_2O condense on frozen SSAs to form nitric acid trihydrate (NAT) particles. As the temperature drops further below approximately 187 K, ice crystals are formed around the NAT particles which now serve as the condensation nuclei. This representation of PSC formation might, however, be too crude or might not apply under all conditions [*Tolbert*, 1994; *Fox et al.*, 1995; *Toon and Tolbert*, 1995]. Observations made by *Schlager et al.* [1990] seem to indicate that liquid SSAs could also serve as condensation nuclei for HNO_3. *Dye et al.* [1992] suggest that sulfate aerosol particles may remain in the liquid phase when the temperature drops below 195 K. In this case, the chemical composition of the aerosol changes as H_2O and HNO_3 molecules are absorbed, and the liquid particles grow as a ternary solution ($H_2SO_4/HNO_3/H_2O$) before crystallizing as NAT particles [*Molina et al.*, 1993]. Finally, as suggested by *Tabazadeh et al.* [1994], the absorption of H_2O and HNO_3 molecules by the ternary solution could lead to amorphous liquid binary solution particles (HNO_3/H_2O) with traces of H_2SO_4. Because the ternary supercooled liquid aerosols grow under much cooler temperatures than NAT, the atmospheric region in which ternary solutions are formed could be smaller than the area in which the NAT produced. More laboratory work and field experiments are needed to improve our understanding of these complex microphysical processes. In this work, we will retain the simple microphysical processes proposed by *Crutzen and Arnold* [1986] and *Toon et al.* [1986].

The purpose of the present paper is to describe a coupled microphysical/chemical/dynamical two-dimensional (2-D) model. As planetary waves produce longitudinal variations in the stratospheric temperature, particularly in the northern hemisphere, polar stratospheric clouds are not distributed uniformly with longitude. This introduces a severe limitation for two-dimensional models which derive zonally averaged quantities, and do not provide explicit information about longitudinal variations. Although microphysical and chemical processes (which are highly nonlinear) should therefore be treated in three-dimensional models, pilot studies may be performed with two-dimensional models if the effects of longitudinal temperature waves are accounted for through some parameterization. Such models are commonly used for assessment studies, and need to account in the best possible way for microphysical processes and heterogeneous chemical reactions. After a description of

Paper number 96JD00404.
0148-0227/96/96JD-00404$09.00

the microphysics model which is coupled to the chemical scheme used in our 2-D model, we will validate the model by comparing calculated PSC distributions with climatology. Part 2 of the present study [*Tie et al.*, this issue] presents several applications of this model.

2. Model Description

The model used in the present study is an updated version of the 2-D (latitude/altitude) chemical/dynamical model of the stratosphere developed by *Brasseur et al.* [1990] and *Granier and Brasseur* [1992]. It extends from pole to pole with a latitudinal resolution of 5° and from the surface to 85 km with a vertical resolution of 1 km. Approximately 60 species and 110 chemical and photochemical reactions are taken into account to describe the behavior of the oxygen, hydrogen, nitrogen, chlorine, bromine, fluorine, and sulfur families [*Brasseur et al.*, 1990]. Heterogeneous processes on sulfate aerosol particles include the following reactions

(R1) $N_2O_5(g) + H_2O(\text{aerosol}) \rightarrow 2\ HNO_3(g)$

(R2) $ClONO_2(g) + H_2O(\text{aerosol}) \rightarrow HNO_3(g) + HOCl\ (g)$

where (g) denotes species in the gas phase. A recent study by Danilin and McConnell (1995) shows that the reactions $BrONO_2$ + H_2O(aerosol) and HOBr + HCl(aerosol) could have significant impact on the chemical species in the lower stratosphere, especially after large volcanic eruptions. These reactions are not included in the current model, but are considered in a separate study (X. Tie and G. Brasseur, The importance of heterogeneous bromine chemistry in the lower stratosphere. Submitted to *Geophysical Research Letters.*, 1995).

The model used to simulate the formation and fate of PSCs is from *Larsen* [1991]. In this microphysical model, the PSC particles are assumed to be spheres, which are distributed within 50 bins according to their size. Radii obey a geometric progression with a ratio of 2. Three types of particles are considered in the model. The first type is represented by diluted sulfuric acid particles, with a size distribution provided by the microphysical model of *Tie et al.* [1994a]. These sulfate aerosol particles serve as cloud condensation nuclei (CCN) for the PSC particles. When the atmospheric temperature decreases, nitric acid vapor becomes supersaturated with respect to NAT [*Crutzen and Arnold*, 1986], and a second type of particle is formed. These particles, named type I PSC particles (PSC I), are composed of a NAT shell surrounding a small sulfate core. When the temperature decreases further and reaches the frost point, PSCs I particles act as condensation nuclei for a third type of particle, named type II PSC (PSC II), composed of an ice shell coating a PSC I core. Particles found in the atmosphere are affected by gravitational sedimentation. Interactions between the particles and the chemical state of the background atmosphere occur through phase changes of water and nitric acid and through heterogeneous reactions on the surface of the aerosol and PSC particles. The three microphysical processes which are considered in the present study, i.e., nucleation, condensation and sedimentation, are briefly described in the following paragraph, while the structure and formation process of the PSCs are schematically represented in Figure 1.

The stratospheric temperatures calculated in the model are usually in fair agreement with temperatures observed at midlatitudes [*Randel*, 1992], but are 10-15 K colder than the observations in the

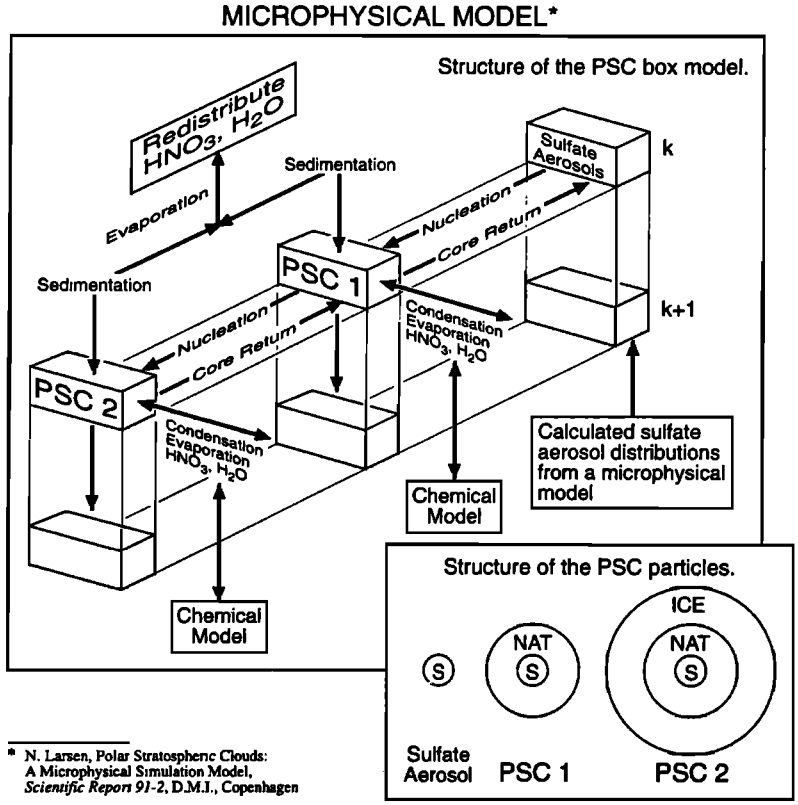

Figure 1. The structure of microphysical processes included in the model [Requirested with the permission from publication by *Larsen*, 1991].

polar regions [*Tie et al.*, 1994b]. Since the formation of PSCs is directly affected by temperature, our microphysical model uses the observed (rather than the calculated) zonal mean temperature measurements (derived from NMC (NOAA National Meteorological Center) made between June 1986 and May 1990. In addition, in order to account for longitudinal variations in the temperature (planetary waves) and the possible processing by PSC air masses flowing through localized cold environments (while the zonal mean temperature may be higher than the PSC thresholds), we have superimposed to the zonal mean temperature $T_m(\varphi)$, a fluctuation $T_w(t,\varphi)$ (hereafter called temperature wave). Thus the temperature used in the microphysical component of the model is expressed as

$$T(t,\varphi) = T_m(\varphi) + T_w(t,\varphi) \quad (1)$$

where t is time and φ is the latitude. In the model the temperature wave is expressed by

$$T_w(t,\varphi) = A(t,\varphi)\ \sin\left(\frac{2\pi U_m t}{a\cos(\varphi)}\right) \quad (2)$$

where U_m is the zonal wind speed (m/sec) calculated in the 2-D model; a is the radius of the earth, and $A(t,\varphi)$ is the amplitude of the temperature wave specified according to *Hitchman and Brasseur* [1988] and *Randel* [1992] (Figure 2).

The key microphysical processes affecting the formation and fate of PSC particles are simulated by the model developed earlier by *Larsen* [1991]. This model assumes that homogeneous nucleation is small and can therefore be ignored. The heterogeneous nucleation rate $J(r)$ of nuclei of radii r is expressed by

$$J(r) = C_m r^2 \frac{P}{kT}\sqrt{\frac{2\sigma Mk}{R\pi\rho^2}}\exp\left(-\frac{\Delta F}{kT}\right) \quad (3)$$

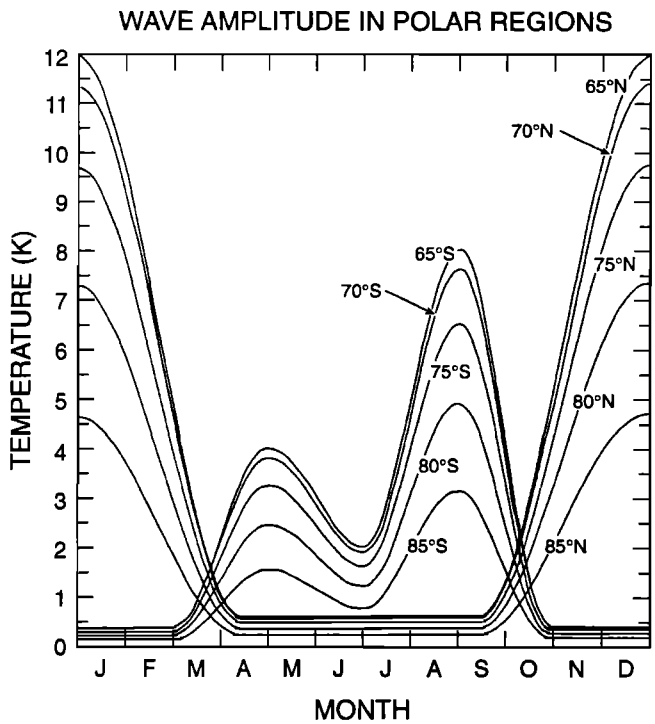

Figure 2. Planetary wave amplitude in polar regions calculated according to *Hitchman and Brasseur* [1988].

where C_m is the number of molecules of water that are absorbed onto surface of the aerosols per area, and is set equal to 2 x 10^{23} m^{-2} [*Larsen*, 1991]; M and P_p are the molar mass and partial pressure of the condensed vapor, r is the radius of the particle, σ and ρ are the surface tension and density of the condensed substance, R is the universal gas constant, T is the atmospheric temperature, k is Boltzmann's constant, and ∇F is the free energy of cluster formation (a compatibility parameter of 0.95 is assumed in the calculation of ∇F). The nucleation rate $J(r)$ is expressed as the number of CCN produced per second. When J(r) is multiplied by the number of condensation nuclei (input from the microphysical model of sulfate aerosols), the product provides the rate of formation of particles at radius $r+\Delta r$; it depends strongly on the saturation ratio and the CCN radius. After large volcanic eruptions, the number density and the average size of aerosol particles increase substantially [*Tie et al.*, 1994a), and hence the nucleation rate of PSC I is enhanced. The impact of volcanic eruptions on the formation of PSCs will be discussed in part 2 of this paper [*Tie et al.*, this issue].

If the HNO_3 vapor pressure is higher than the saturation pressure for NAT particles, condensation occurs and PSC I particles grow to larger sizes. In the model, the rate of condensation *dm/dt* is expressed according to Pruppacher and Klett [1980]:

$$\frac{dm}{dt} = \frac{4\pi f_v CDM}{R}\left(\frac{P}{T} - \frac{P_s}{T_r}\right) \quad (4)$$

where m is the mass of the condensed substances per unit volume of air; T_r is the temperature at the particle surface, D is a diffusion coefficient, $C=C_c r$ is the "capacity" of the particle, C_c=1.16 [*Pruppacher and Klett*, 1980], f_v is the ventilation factor, arising because the particles fall. P and P_s are the vapor pressure and saturation pressure for the particles in the atmospheric environment. The surface temperature T_r is calculated from the release or uptake of latent heat during condensation or evaporation. If $P/T - P_s/T_r$ *is* greater than zero, particles condense and grow. Otherwise, they evaporate and shrink. A similar expression is used for the condensation/evaporation of PSC II. The saturation pressure (P_s) for PSC I and PSC II is critical to determine the fate of the particles. For nitric acid over PSC I particles, P_s is calculated from the expression given by *Hanson and Mauersberger* [1988], while for water vapor over PSC II particles, it is taken from *Jancso et al.* [1970]. A recent study by Marti and *Mauersberger* [1993] shows that the treshold temperature for the formation of PSC II could be 20% lower, leading to fewer PSC II clouds in the polar regions.

When the size of the particles becomes large, gravitational sedimentation becomes important, and the particles are transported downward from the stratosphere into the troposphere. As a consequence, nitric acid and water vapor are removed from the stratosphere, a process called "denitrification and dehydration". In addition, when the particles reach layers where the temperature is sufficiently high to produce evaporation, particles are converted back into nitric acid and water vapor. The net effect of sedimentation is therefore to transport nitric acid and water vapor from higher levels (15-22 km) to lower levels (8-15 km). The sedimentation process is determined by the terminal fall velocity U, given by *Fuchs* [1964]

$$U = \frac{2\rho r^2 g}{9\eta K}\left[1 + 1.246\frac{L_a}{r} + 0.42\frac{L_a}{r}\exp\left(-0.87\frac{r}{L_a}\right)\right] \quad (5)$$

where L_a is the mean free path of the air molecules, η is the

dynamic viscosity of air, g (=9.8 m/s^2) is the gravitational acceleration; r is the radius of particles, and K =1.12 is the dynamic shape factor.

Microphysical coagulation through which particles collide and attach to each other to form larger particles is not, according to the studies by *Toon et al.* [1989] and *Larsen* [1991], a significant process for PSC particles, due to their low number density. Coagulation has therefore been ignored in the present study.

With these processes taken into account, the model provides an estimate as a function of time of the particle size distribution and thereby of the surface area available for heterogeneous reactions in PSCs. The heterogeneous reactions included in the model are the following:

(R3) $ClONO_2(g) + H_2O(s) = HOCl(g) + HNO_3(s)$
(R4) $ClONO_2(g) + HCl(s) = Cl_2(g) + HNO_3(s)$
(R5) $N_2O_5(g) + H_2O(s) = 2\,HNO_3(s)$
(R6) $N_2O_5(g) + HCl(s) = ClNO_2(g) + HNO_3(s)$
(R7) $HOCl(g) + HCl(s) = Cl_2(g) + H_2O(s)$

where (g) denotes the species in the gas phase and (s) species in the condensed (liquid or solid) phase. The kinetic rates of these five reactions depend on the mean speed (v) of the gaseous molecules (calculated as a function of the temperature and molecular weight) and on the available particle surface area (A). They are expressed by equivalent first-order rate constants as $k=\gamma vA/4$, where γ is the reaction probability provided by laboratory measurements for each of the five processes (R3)-(R7). The values of the accommodation coefficients of γ used in the calculation are listed in Table 1.

3. Simulation of PSCs

In order to estimate the rate of heterogeneous reactions (R3)-(R7), it is first necessary to assess the formation of PSC I and PSC II, to calculate the corresponding surface area density, and to derive the impact of these clouds on the abundance of gas phase compounds, such as HNO_3 and water vapor. To illustrate the results provided by the PSC microphysics model, we will first show detailed output at two given grid points of the model: 21-km altitude at 75°N and 75°S, respectively. Figure 3 shows the evolution of the temperature (with the wave taken into account) during winter and spring at these 2 locations. In the northern hemisphere the temperature oscillates between approximately 192 K and 208 K during January. The threshold for PSC I formation (194.5 K) is reached; the threshold (186 K) for PSC II formation is never encountered. In the southern hemisphere, PSC I are formed between June and the end of November, while PSC II are produced episodically between mid-August and the end of September. The corresponding surface area density is shown in Figure 4 for PSC I and II, respectively. If

Table 1. Reaction Probabilities Used in the Model

	PSC II	PSC I
$ClONO_2 + H_2O$	0.3*	0.006*
$ClONO_2 + HCl$	0.3**	0.3*
$N_2O_5 + H_2O$	0.024*	0.0006*
$N_2O_5 + HCl$	0.05**	0.032*

* *Hanson and Ravishankara* [1991]
** *Leu* [1988]

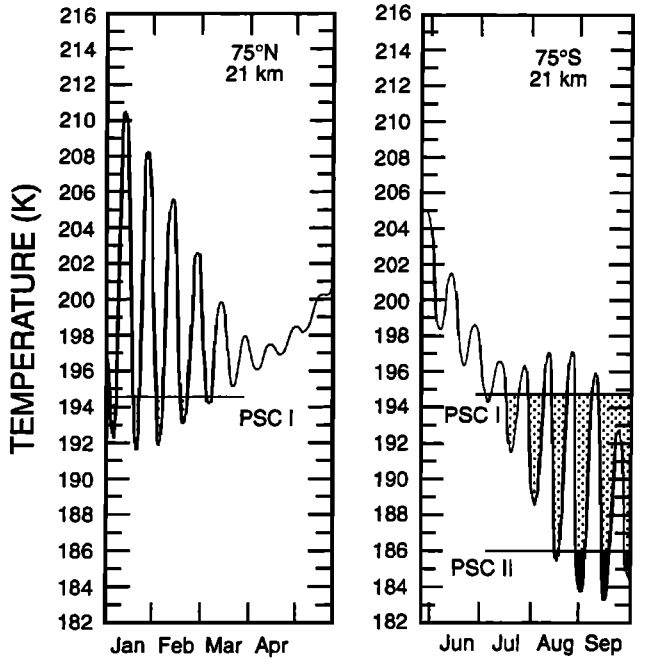

Figure 3. Evolution of the temperature with planetary waves taken into account, used to calculate the formation of PSCs at 21 km at 75°N and 75°S.

averaged over a period of 15 days (which corresponds to the time step used in the model for the transport of tracers, the mean surface area for PSC I reaches approximately 2.5 μ m^2/cm^3 during January and February in the northern hemisphere (21 km, 75°N), and 7-8 μ m^2/cm^3 between September and November in the southern Hemisphere (21 km, 75°S). The surface area associated with PSC II is approximately 1 μ m^2/cm^3 in southern hemisphere (21 km,

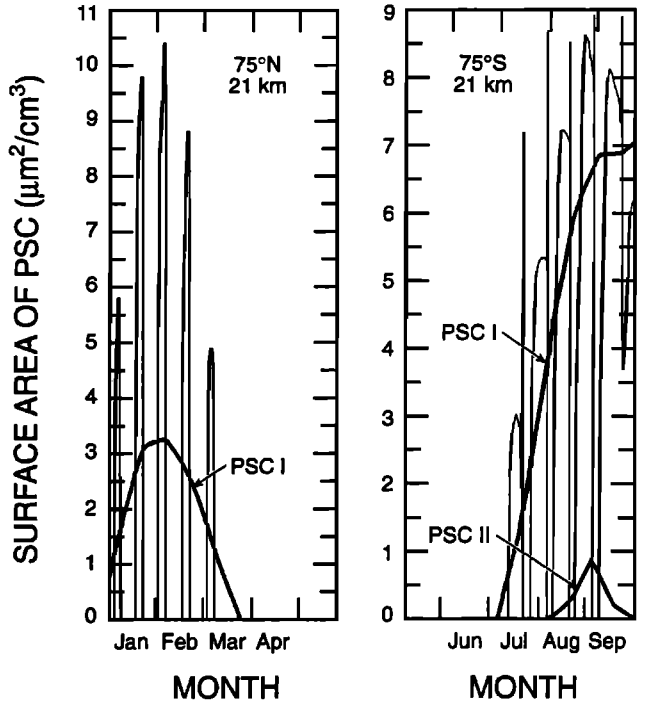

Figure 4. Calculated evolution of the surface area density (μ m^2/cm^3) of type I and II PSCs at 21km at 75°N and 75°S.

75°S). The role of PSC II is, however, very important, as the largest particles (predicted to be formed only in the southern hemisphere) are subject to gravitational sedimentation and provide a loss mechanism for stratospheric H_2O and HNO_3. Figures 5a and 5b show the evolution of the gas phase H_2O and HNO_3 mixing ratios, as predicted by the model. Superimposed on the instantaneous calculated values are the 15-day averaged mixing ratios. The effect of sedimentation is most visible at 75°S in September, but is negligible at 75°N.

The zonally averaged distribution of the surface area density associated with PSC I in the Antarctic winter, as provided by microphysics model for three different time periods (average over 15 days) is shown in Figure 6. Because the zonally averaged winter temperature over Antarctica remains below the threshold temperature (approximately 195 K) for PSC I formation between July and September (see Randel, 1992), type I particles exist persistently in winter from 10- to 20-km altitudes, south of 65°S. This result is consistent with observations made between 1978 and 1985 and reported by *McCormick and Trepte* [1987], and *Poole and Pitts* [1994]. In mid-August, for example, the maximum in the surface area is about 9 $\mu m^2/cm^3$ (see Figure 6a), while, in late August, it increases to approximately 15 $\mu m^2/cm^3$ (see Figure 6b). In September, as the temperature increases slowly, the surface area density starts to decrease. Type I particles are first being evaporated at the top of the cloud (around 20 km) and the maximum surface area density is reduced to 9 $\mu m^2/cm^3$ in mid-September.

In the case of type II particles, the threshold temperature is approximately 187 K, which is usually below the observed zonally averaged temperature in Antarctica during winter. In this case, the temperature wave plays a more significant role. In our model simulation, PSC II exist only during a short time with a distribution which is more complex than in the case of PSC I (see Figure 7). For example, in early August there is no type II cloud, while a type I cloud is well developed. In late August the occurrence of PSC II reaches a maximum (with a highly irregular distribution). and in mid-September most PSC II particles have evaporated or sedimented; only a small amount remains in the lower stratosphere (below 15 km).

Figure 8 shows a prediction of the PSC occurrence during the Antarctic winter compared with the observations of *McCormick*

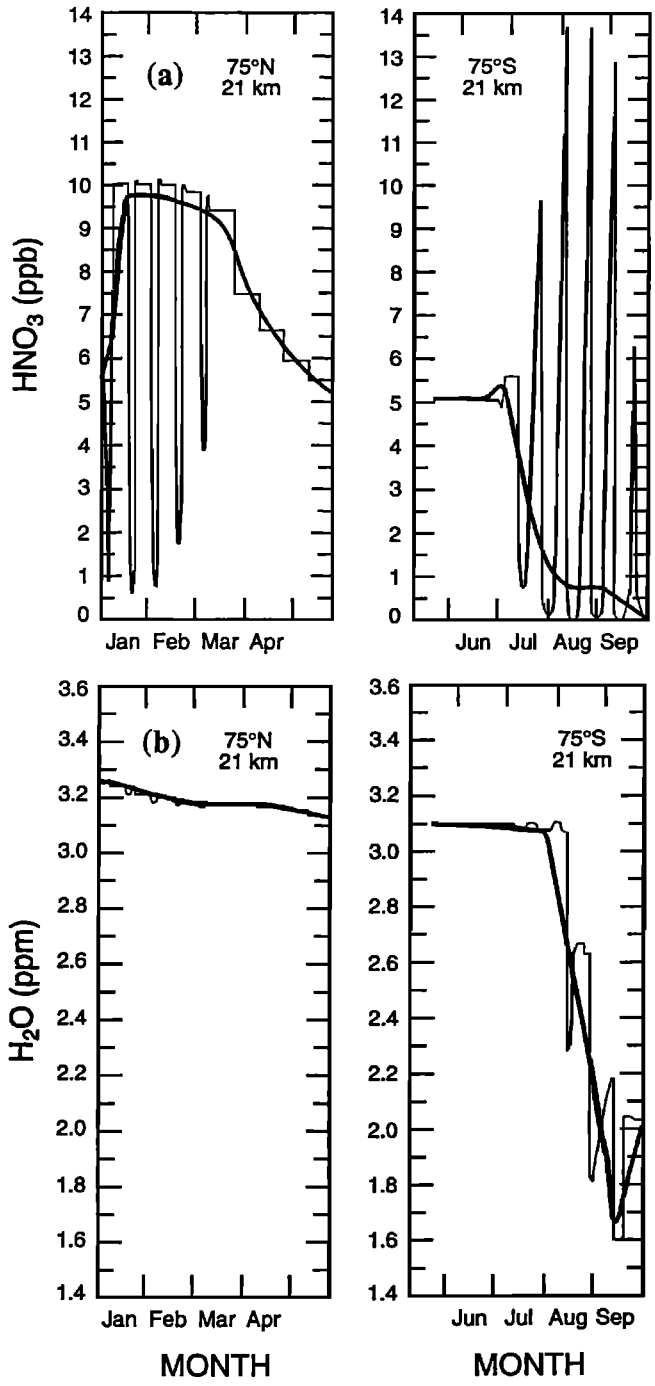

Figure 5. Calculated concentration of (a) HNO_3 (ppb) and (b) H_2O (ppm) at 21 km at 75°N and 75°S with condensation effects taken into account.

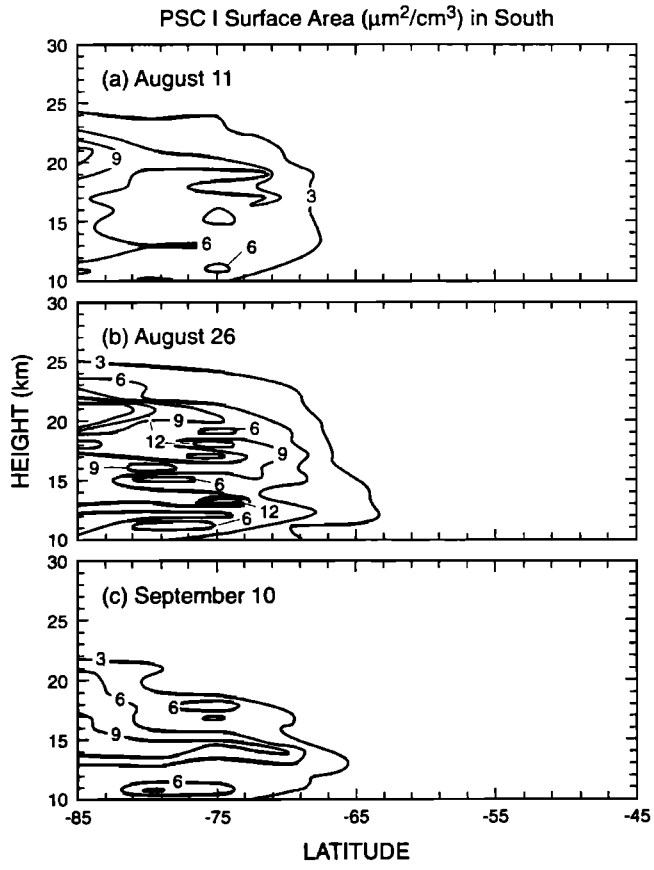

Figure 6. Calculated surface area ($\mu m^2/cm^3$) distribution of PSC I in the southern hemisphere during winter-spring.

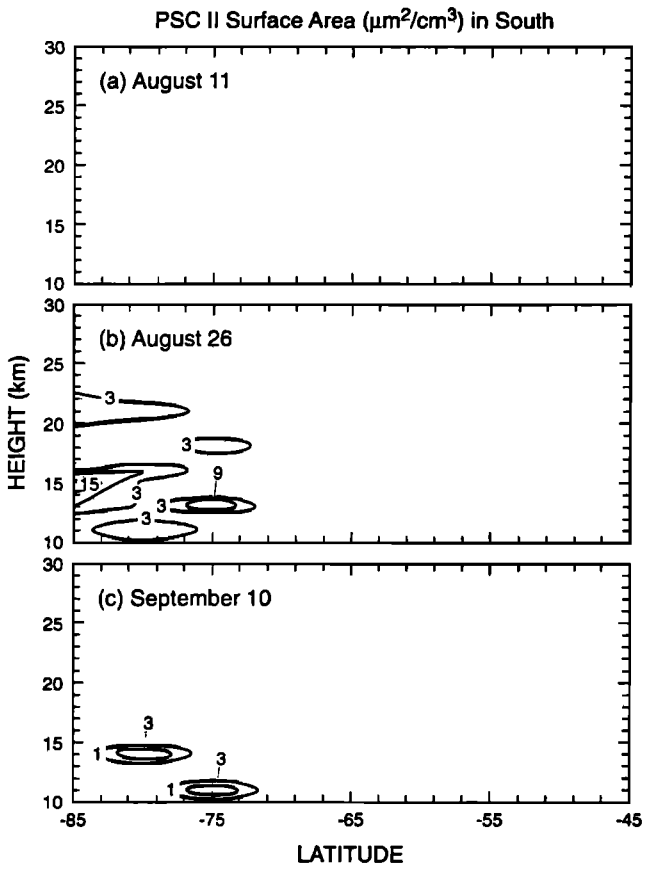

Figure 7. Same as Figure 6 except distribution is for PSC II.

and Trepte [1986]. Because the quantities are different in each case (surface area for the calculation versus extinction ratio for the observations), we only attempt to compare the timing, location, and relative density of the PSCs. First, both the observations and calculations show the presence of PSCs between 10- and 25-km altitudes from early June to late September. Second, the model reproduces fairly well the temporal evolution of the PSC. The calculated PSC density is, for example, very small in May and significantly increases in late June; it increases further in July and August, then starts to decrease in September, and almost disappears in October. Third, the density of the PSC particles varies similarly in the model and in the observations. The large amount of PSCs predicted above 17 km in July/August disappears in September, consistent with the observation of *McCormick and Trepte,* [1987]. Measured extinction ratios remain, however, significant in late September and in October below 15 km, while no PSCs are predicted by the model after September 15 in this altitude range. The observed as well as calculated distributions of PSCs are complex, which suggests that the temperature wave has an important effect on the distribution of the PSCs. Observations also show a correlation in the timing of the PSC occurrence and low temperatures [*Poole and Pitts,* 1994].

In the Arctic where the average temperature is higher than in the Antarctic, the formation of PSCs is different from that in the vicinity of the south pole. The mean temperature is usually higher than the threshold temperature for PSC I [*Randel,* 1992; *McCormick and Trepte*, 1987]. However, the temperature wave at middle to high latitudes is sufficiently strong [*Hitchman and Brasseur,* 1988] to produce occasionally localized regions with sufficiently cold air masses in which PSC I is produced (see Figure 2).

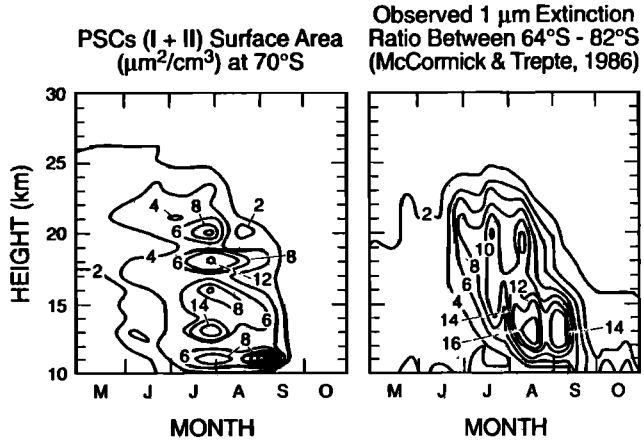

Figure 8. Comparison between calculated and observed [*McCormick and Trepte,* 1986] altitude-time distribution of PSCs at 70°S in the lower stratosphere. Calculated surface areas are in $\mu m^2/cm^3$. Observations are expressed as 1-μm extinction ratios.

The calculated surface area of PSC I particles in the Arctic, shown in Figure 9, is approximately 5-10 times smaller than in Antarctica (see Figure 6); this result is consistent with the observation of the sighting density in both polar regions [*World Meteorological Organization (WMO),* 1991]. Furthermore, the maximum surface area in the northern hemisphere is often found between 65°N and 75°N, and not at the pole, as in Antarctica. This difference between hemispheres is explained by the strong temperature wave observed

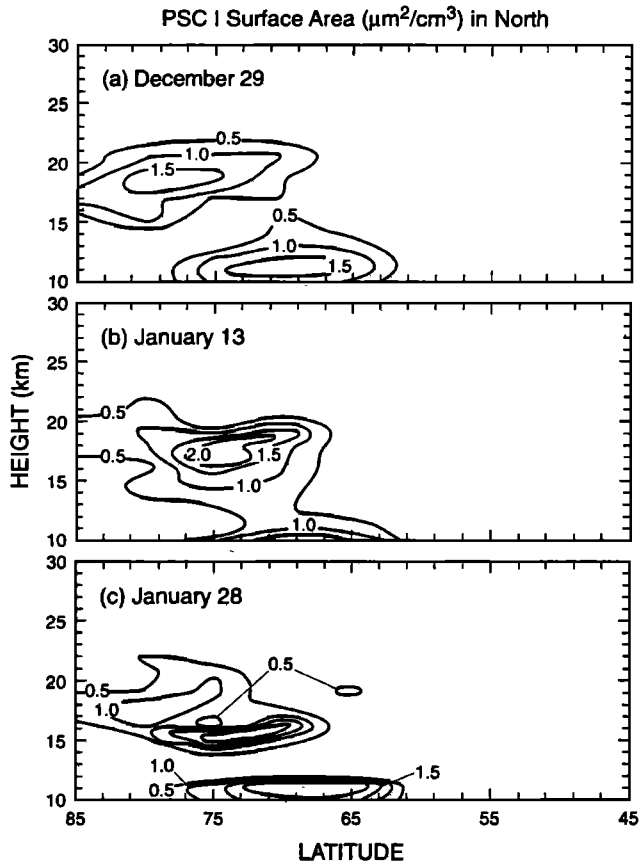

Figure 9. Calculated surface area ($\mu m^2/cm^3$) distribution for PSCs I at 70°N in winter.

between 65°N and 75°N. PSC events occurring near the edge of the vortex have been observed during the Airborne Arctic Stratospheric Expedition (AASE) and reported by *Dye et al.* [1990]. *Schoeberl and Hartmann* [1991] explained the PSC events by the cooling of air by an upward bulge near the tropopause produced by tropospheric cyclones. This bulge acts like an orographic feature and results in adiabatic expansion, cooling, and the formation of stratospheric clouds.

Finally, Figure 10 shows that, at 70°N, type I PSCs exist from mid-December to mid-February, i.e., during a time period that is much shorter than in Antarctica (from May to late September, see Figure 8). This model result is in agreement with the observations except between 10 and 12 km where the calculated surface area is slightly higher than suggested by the observations [*WMO*, 1991; *Poole and Pitts*, 1994].

In conclusion, the simulated zonally averaged distributions of PSCs in both Antarctica and in the Arctic are consistent with observations, despite the limitations inherent to two-dimensional models. In the part 2 of this paper, we will examine how the calculated surface areas provided by the PSCs affect the chemical composition of the lower stratosphere, including ozone.

4. Summary and Conclusion

A two-dimensional chemical-dynamical-radiative model of the middle atmosphere has been coupled to a microphysical model to study the formation and the evolution of PSCs, and their impacts on stratospheric ozone in Antarctica and in the Arctic. The calculation shows that PSC distributions can be well represented in a two-dimensional model if the effect of planetary waves on the temperature is explicitly taken into account. Type I PSCs exist from early June to late September over Antarctica with a maximum surface area of approximately 25 $\mu m^2/cm^3$. Type II PSCs are present for a much shorter time (mainly in August), with an irregular spatial structure. In the Arctic, no PSCs II are produced in the model, and surface areas of PSCs I are approximately 5 times smaller than in Antarctica. Because the temperature wave is a dominant factor for the formation of PSCs I, these latter clouds are found at edge of the Arctic vortex where the wave amplitude is largest and its period shortest (mainly in January).

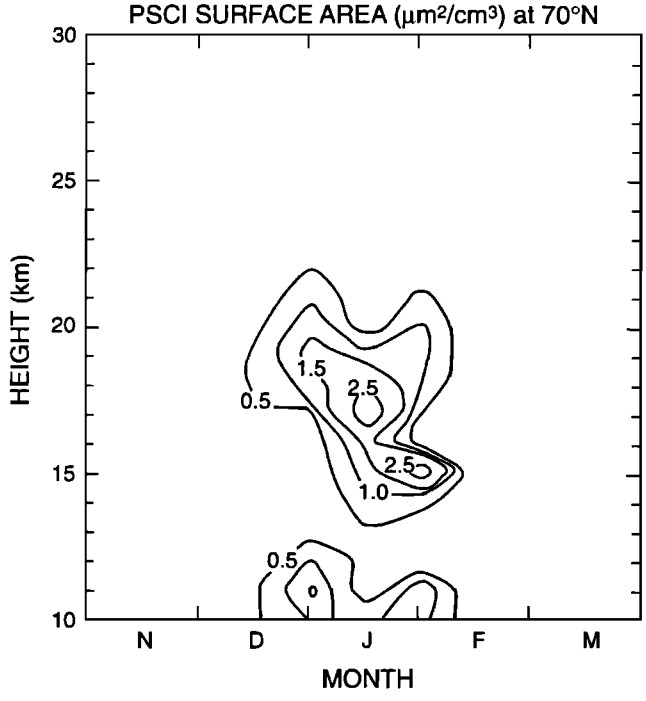

Figure 10. Calculated altitude-time distribution of surface area ($\mu m^2/cm^3$) of PSC I at 70°N in the lower stratosphere.

Acknowledgments. The authors are grateful to Anne Smith, Steve Massie, Andrew Weinheiimer, and two anonymous reviewers for useful comments on the manuscript. This research was supported in part by the Commission of European Communities (Environment Program). X. Tie and G. Brasseur were supported in part by the U.S. Department of Energy under contract DE-AI05-94ER619877. Claire Granier is supported by the Gas Research Institute (contract 5090-254-1993). Guy Brasseur is supported in part at the University of Brussels by the Global Change program of the Belgian government under contract GC/11/018/. The National Center for Atmospheric Research is sponsored by the National Science Foundation.

References

Brasseur, G., M. H. Hitchman, S. Walters, M. Dymek, E. Falise, and M. Pirre, An interactive chemical dynamical radiative two-dimensional model of the middle atmosphere, *J. Geophys. Res., 95,* 5639-5655, 1990.

Crutzen, J. P., and F. Arnold, Nitric acid cloud formation in the cold Antarctic stratosphere: A major cause for the springtime "ozone hole", *Nature, 324,* 651-655, 1986.

Danilin, M. Y., and J. C. McConnell, Stratospheric effects of bromine activation on/in sulfate aerosol, *J. Geophys. Res., 100,* 11,237-11,243,1995.

Dye, J. E., B. W. Sandred, D. Baumgardber, L. Sanford, and G. V .Ferry, A survey of particle measurements in the Arctic from the forward Scattering spectrometer probe model 300, *Geophys. Res. Lett., 17,* 409-412, 1990.

Dye, J. E., D. Baumgardner, B. W. Gandrud, S. R. Kawa, K. K. Kelly, M. Loewenstein, G. V. Ferry, K. R. Chan, and B. L. Gary, Particle size distributions in Arctic polar stratospheric clouds, growth and freezing of sulfuric acid droplets, and implications for cloud formation, *J. Geophys. Res., 97,* 8015-8034, 1992.

Fox, L. E., D. R. Worsnop, M. S. Zahniser, and S. C. Wofsy, Metastable phases in polar stratospheric aerosols, *Science, 267,* 351-355, 1995.

Fuchs, N. A., *The Mechanics of Aerosols,* 408 pp, Pergamon Press, New York, 1964.

Granier, C. and G. Brasseur, Impact of heterogeneous chemistry on model predictions of ozone changes, *J. Geophys. Res., 97,* 18,015-18,033, 1992.

Hanson, D., and K. Mauersberger, Laboratory studies of the nitric acid trihydrate: Implications for the south polar stratosphere, *Geophys. Res. Lett., 15,* 855-858, 1988.

Hanson, D. R., and A. R. Ravishankara, The reaction probabilities of $ClONO_2$ and N_2O_5 on Polar Stratospheric Cloud Materials, *J. Geophy. Res., 96,* 5081-5090, 1991.

Hitchman, M.H., and G. Brasseur, Rossby wave activity in a two-dimensional model: Closure for wave driving and meridional eddy diffusivity, *J. Geophys. Res., 93,* 9,405-9,417, 1988.

Jancso, G., J. Pupezin, and W. A. Van Hook, The vapor pressure of ice between $+10^{-20}$ and 10^{20}, *J. Phys. Chem., 74,* 2984-2989, 1970.

Larsen, N., Polar stratospheric clouds: A microphysical simulation model, *DMI Sci. Rep. 91-2,* Dan. Meteorol. Inst., Copenhagen, 1991.

Leu, M. T., Laboratory studies of sticking coefficients and heterogeneous reactions important in the Antarctic stratosphere, *Geophys. Res. lett., 15,* 17-20, 1988.

Marti, J., and K. Mauersberger, A survey and new measurements of ice vapor pressure at temperatures between 170 and 250K, *Geophys. Res. Lett., 20,* 363-366, 1993.

McCormick, M. P., and C. R. Trepte, SAM II measurements of Antarctic PSC and Aerosols, *Geophys. Res. Lett., 13,* 1276-1279, 1986.

McCormick, M. P., and C. R. Trepte, Polar stratospheric optical depth observed between 1978 and 1985, *J. Geophys. Res. 92,* 4297-4306, 1987.

McCormick, M. P., H. M. Steele, P. Hamill, W. P. Chu, and T. J. Swissler, Polar stratospheric cloud sights by SAM II, J. Atmos. Sci., 39, 328-331, 1982.

McCormick, M. P., P. Hamill, and U. O. Farrakh, Characteristics of polar stratospheric cloud as observed by SAM II, SAGE, and lidar, J. Metorol. Soc. Jpn., 63, 267-276, 1985

Molina, M. J., R. Zhang, P.J. Wooldridge, J. R. McMahon, J. E. Kim, H. Y. Chang, and K. Beyer, Physical chemistry of the $H_2SO_4/HNO_3/H_2O$ system: Implications for polar stratospheric clouds, *Science, 261,* 1418, 1993.

Poole, L. R., and P. McCormick, Polar stratospheric clouds and Antarctic ozone hole, *J. Geophys. Res., 93,* 8423-8430, 1988.

Poole, L. R., and M. C. Pitts, Polar stratospheric cloud climatology based on Stratospheric Aerosol Measurement II observations from 1978 to 1987, *J. Geophys. Res., 99,* 13,083-13,089, 1994.

Pruppacher, H. R., and J. D. Klett, *Microphysics of Clouds and Precipitation,* 2nd ed., 714 pp, D. Reidel, Newell, Mass. 1980.

Randel, W. J., Global atmospheric circulation statistics, 1000-1 mb, *NCAR Tech. Note TN-366,* Natl. Cent. for Atmos. Res., Boulder, Colo., 1992.

Schlager, H., F. Arnold, D. Hofmann, and T. Deshler, Balloon observations of nitric acid aerosol formation in the Arctic stratosphere, I, Gaseous nitric acid, *Geophys. Res. Lett., 17,* 1275-1278, 1990.

Schoeberl, M. R., and D. L. Hartmann, The dynamics of the stratospheric polar vortex and its relation to springtime ozone depletions, *Science, 251,* 46-52, 1991.

Tabazadeh, A., R. P. Turco, K. Drdla, and M. Z. Jacobson, A study of type I polar stratospheric cloud formation, *Geophys. Res. Lett., 21,* 1619-1622, 1994.

Tie, X., X. Lin, and G. Brasseur, Two-dimensional coupled dynamical/chemical/microphysical simulation of global distribution of El Chichon volcanic aerosols, *J. Geophys. Res., 99,* 16,779-16,792, 1994a.

Tie, X., G. P. Brasseur, B. Briegleb, and C. Granier, Two-dimensional simulation of Pinatubo aerosol and its effect on stratospheric ozone, *J. Geophys. Res., 99,* 20,545-20,562, 1994b.

Tie, X., G. P. Brasseur, C. Granier, A. De Rudder, and N. Larsen, Model study of polar stratospheric clouds and their effect on stratospheric ozone, 2, Model results, *J. Geophys. Res.,* this issue.

Tolbert, M. A., Sulfate aerosols and polar stratospheric cloud formation, *Science, 264,* 527-528, 1994.

Toon, O. B., and M. A. Tolbert, Spectroscopic evidence against nitric acid trihydrate in polar stratospheric clouds, *Nature, 375,* 218-220, 1995.

Toon, O. B., P. Hamill, R. P. Turco, and J. Pinto, Condensation of HNO3 and HCl in the winter polar stratospheres, *Geophys. Res. Lett., 13,* 1284-1287, 1986.

Toon, O. R. P. Turco, J. Jordan, J. Goodman, and G. Ferry, Physical processes in polar stratospheric ice clouds, *J. Geophys. Res. 94.,* 11359-11380, 1989.

Toon, O. B., R. P. Turco, and P. Hamill, Denitrification mechanisms in the polar stratospheres, *Geophys. Res. Lett., 17,* 445-448, 1990.

Turco, R. P., O. B. Toon, and D. Hamill, Heterogeneous physicochemistry of the polar ozone hole, *J. Geophys. Res., 94,* 16493-16510, 1989.

World Meteorological Organization, *Scientific Assessment of Ozone Depletion: 1991,* Geneva, 1991.

Anne De Rudder, CNRM, Meteo-France, 42, avenue Gustave Coriolis, F - 31057 Toulouse, France.

Niels Larsen, Division of Middle Atmospheric Research, Danish Meteorological Institute Lyngbyvej 100, DK-2100 Copenhagen, Denmark.

Guy P. Brassuer, Claire Granier, and Xuexi Tie, National Center for Atmospheric Research Boulder, Colorado 80307.

(Received April 19, 1995; revised November 16, 1995; accepted January 5, 1996.)